



HAL
open science

Specifications for carbonate content quantification in recent marine sediments using Rock-Eval pyrolysis.

Adrien Wattripont, François Baudin, Marc de Rafélis, Jean-François Deconinck

► To cite this version:

Adrien Wattripont, François Baudin, Marc de Rafélis, Jean-François Deconinck. Specifications for carbonate content quantification in recent marine sediments using Rock-Eval pyrolysis.. *Journal of Analytical and Applied Pyrolysis*, 2019, 140, pp.393-403. 10.1016/j.jaap.2019.04.019 . hal-02140273

HAL Id: hal-02140273

<https://hal.science/hal-02140273v1>

Submitted on 22 Oct 2021

HAL is a multi-disciplinary open access archive for the deposit and dissemination of scientific research documents, whether they are published or not. The documents may come from teaching and research institutions in France or abroad, or from public or private research centers.

L'archive ouverte pluridisciplinaire **HAL**, est destinée au dépôt et à la diffusion de documents scientifiques de niveau recherche, publiés ou non, émanant des établissements d'enseignement et de recherche français ou étrangers, des laboratoires publics ou privés.



Distributed under a Creative Commons Attribution - NonCommercial 4.0 International License

1 Specifications for carbonate content quantification in recent marine sediments using Rock-Eval pyrolysis

2

3

4 Adrien Wattripont^{1,2}, François Baudin¹, Marc de Rafelis^{1,3} and Jean-François Deconinck⁴

5

6 ¹ Sorbonne Université, CNRS, IStEP, 4 place Jussieu 75005 Paris, France7 ² Vinci-Technologies, 27b rue du Port, 92000 Nanterre, France8 ³ Present address: GET, Université de Toulouse, CNRS, IRD, UPS, 31400 Toulouse, France9 ⁴ Université de Bourgogne Franche-Comté, CNRS, Biogéosciences, 6 bd Gabriel, 21000 Dijon, France

10

11 Corresponding author: francois.baudin@sorbonne-universite.fr

12

13 Abstract

14

15 The amount of CaCO₃ in sediments and/or sedimentary rocks is usually measured by calcimetry while the
16 nature of the carbonates is determined by X-ray diffraction. Recently, a carbonate recognition method based on
17 the results of Rock-Eval pyrolysis was proposed in 2014 by Pillot *et al.* [1]. Rock-Eval pyrolysis is also widely
18 used for the characterization of recent sediments. However, later in 2015 Baudin *et al.* [2] noticed that some of
19 the characteristics of recent sediments tended to produce different results from those of more classical Rock-
20 Eval analyses, causing bias in interpretations.

21 In this study, the thermal stability of fossil and recent marine carbonated sediments was analyzed to identify
22 differences in carbonate decomposition and to underline the importance of accounting for them in Rock-Eval
23 analyses. The state of calcite preservation in recent marine sediments and sedimentary rocks at temperatures
24 between 400 °C and 600 °C was characterized using different techniques (calcimetry, XRD, SEM imaging,
25 etc.) for better interpretation of data obtained with Rock-Eval.

26 Our results highlight a clear difference in the range of calcite decomposition temperatures during Rock-Eval
27 analysis: between 550 °C and 775 °C for bulk clayey hemipelagic sediments versus 650 °C to 840 °C after the
28 same sediments were rinsed to get rid of the salt. During heating, water and hydroxide anions are released from
29 clay minerals and react with salt crystals to form acid vapor. This acid vapor reacts with carbonates to produce
30 CO₂. The chemical decomposition of carbonate starts at temperatures that are lower than the typical range of
31 decomposition temperatures, leading to overestimation of mineral carbon content (overestimation of the S5
32 peak) and to underestimation of organic carbon content (underestimation of the S4CO₂ peak) with the Rock-
33 Eval method. In the absence of clay minerals, such as in recent marine pure carbonate oozes, there is no
34 evidence for this effect. It is therefore essential to prepare and rinse recent clay-rich carbonated sediment
35 samples before Rock-Eval analysis to avoid misinterpretation.

36

37 Keywords

38

39 Rock-Eval - Pyrolysis - Recent sediments - Carbonates decomposition - Acid attack

40

41 Introduction

42

43 The abundance of carbonates in rocks, sediments and soils is an important parameter for many geological,
44 pedological and environmental studies. Several approaches enable the evaluation of the carbonate content in
45 selected samples, including wet chemical dissolution, spectral techniques, and analysis of gas that evolves
46 during thermal decomposition. For wet-chemistry, total carbonate content is determined via acid digestion of
47 the various carbonate minerals (calcite, dolomite, siderite, ankerite, rhodochrosite, etc.) present in the sample.
48 Hydrochloric acid is usually used at room temperature or under moderate heating, to digest the carbonate
49 minerals. Total carbonate contents are determined by measuring either (1) the weight loss of the sample after
50 decarbonation, (2) the acid consumption needed for the complete destabilization of carbonates, or (3) CO₂
51 pressure during decarbonation using a Bernard calcimeter or a Mélières manocalcimeter.

52

53 Rock-Eval analyses are also widely used in the petroleum industry because they make it possible to obtain the
54 percentage of organic matter in a rock and many other parameters that are useful for the characterization of oil
55 potential. The Rock-Eval method was primarily developed by the *Institut Français du Pétrole* for compacted
56 (fossil) sediments [3,4] but is now being increasingly used for the characterization of recent lacustrine and
57 marine sediments [5,6,7,8,9,10,11,12,13,14,15,16,17,18,19,20 and others] as well as soils

58 [21,22,23,24,25,26,27 and others]. In 2014, a qualitative and quantitative carbonate recognition method based
59 on the results of Rock-Eval pyrolysis was proposed [1]. According to this method the morphology of the CO₂
60 production curve obtained during thermal destabilization of carbonated minerals also allows the identification
61 of the type of carbonates present in the rock.

62
63 However, in a previous study [2] we demonstrated that for Rock-Eval analyses of some recent marine
64 sediments are biased, which can lead to misinterpretation of the results (organic matter and / or carbonate
65 content). The aim of the present study was thus to identify the cause of the differences in recent marine
66 sediments. The stability of recent carbonate natural samples subjected to heat treatment (such as those used in
67 Rock-Eval pyrolysis) was compared to the same sample set but previously desalted.
68 In parallel, different sample characterization techniques (calcmetry, XRD, scanning electron microscope
69 imaging, etc.) were carried out to insure a better interpretation of the data obtained by the Rock-Eval and to
70 propose specific conditions for analysis and/or the preparation of recent sediments.
71

72 73 **1. Materials and methods**

74 **1.1 Material**

75
76 As the purpose of this study was to understand the thermal behavior of carbonates in recent sediments, we
77 chose samples of different sedimentary rocks with similar carbonate composition (content, mineralogy) to
78 better identify the origin of the phenomenon. We chose consolidated sedimentary rock samples, recent clay-rich
79 sediment samples and pure carbonate ooze samples. The following samples were analyzed:
80

81 **Douvrend**

82 Douvrend corresponds to the last fifteen centimeters of the upper Cenomanian "Craie de Rouen" Formation
83 (Marnière de Douvrend section, Renouval Quarry, Dieppe region, France). It is a white to light beige marly
84 chalk mainly made of coccoliths and foraminifera. It contains very little organic matter (TOC<0.3%) and is
85 characterized by approximately 90.42±2% CaCO₃ (calcite) content [28]. The sample is in the form of a
86 homogeneous powder and used as IStEP laboratory internal standard for stable carbon and oxygen isotope
87 measurements and trace element analyses.
88

89 **MD01-2376 core**

90 The MD01-2376 core was taken in the Timor Sea (12.314°S, 121.192°E) at a depth of 2906 m below the
91 surface during the IMAGES VII MD122 (WEPAMA) cruise in May 2001 and penetrated the sediment to a
92 depth of 27.90 m. Based on visual examination and smear slide observations the sediment is composed of a
93 siliceous (10-30% diatomaceous) and carbonated (20-45% coccoliths and foraminifera) biogenic phases, clay
94 minerals (25-45%) and organic matter (~ 1%). The color of the sediment (sometimes bioturbated) varies from
95 light to olive gray [29].
96 Since its recovery and opening, the MD01-2376 core has been stored in the cold and humid core repository of
97 the French National Museum of Natural History in Paris. Around 5 cc of wet sediment were collected at
98 approximately 10 cm intervals along the MD01-2376 core from its top down to 27.90 m (260 samples). Three
99 larger samples (15 cc corresponding to a 2 cm thick interval) were collected at different depths of the core: 464-
100 466 cm, 1914-1916 cm and 2345-2347 cm, in order to dispose of a sufficient quantity of material for additional
101 analyses (see below). In the present paper, samples from this core are hereafter referred to as "bulk clayey
102 hemipelagic ooze" and "rinsed clayey hemipelagic ooze", respectively.
103

104 **SU90-08 core**

105 These samples were collected from the top of the core (0.2 first meters) extracted with the Suroît (Ifremer)
106 research vessel in 1990 during the PALEOCINAT drilling campaign at a depth of 3080 m below the surface
107 north of the Azores (43.353N, -30.408W), in the Atlantic Ocean [30,31]. The pelagic sediment in this zone is
108 characterized by approximately 90% calcite content, low TOC (<0.2%) and a very small proportion of clay
109 minerals. Samples from this core are hereafter referred to as "nannofossil pelagic ooze".
110

111 **1.2 Methods**

112

113 The first batch of sediment was dried at 50 °C in a stove and then crushed with an agate mortar. The second
114 batch was rinsed twice in deionized water to remove residual salt from marine pore water. Conductivity was
115 measured to insure the rinses were effective. The samples were then centrifuged and finally dried in a stove at
116 50 °C for 10 hours. We believe that this rinsing has no influence on the carbonate content because the
117 procedure is fast (2 minutes maximum before centrifugation) and made with a neutral pH water.

118

119 **Off-line thermal decomposition**

120 Both bulk and rinsed samples were subjected to the following thermal protocol:

- 121 - 11 mid-ramp isothermal sections in increments of 20 °C (from 400 °C to 600 °C) at 30 min intervals;
- 122 - Each powdered sample was divided into 11 aliquots each weighing 0.6 g;
- 123 - The aliquots were placed together in a muffle furnace at ambient temperature and ambient air
124 atmosphere;
- 125 - The furnace was then heated to 400 °C;
- 126 - Then, for each isothermal section, the temperature was stabilized for 30 minutes;
- 127 - At the end of each isothermal section, an aliquot was removed from the oven, cooled and weighed.

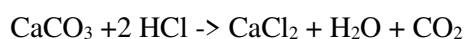
128 This protocol was repeated for each sample, and a total of 60 aliquots (including raw samples) were prepared
129 and analyzed.

130

131 **Calciometry**

132 The measuring instrument used in this study was a Mélières manocalcimeter. The calcium carbonate dosage is
133 based on acid attack (here with 30% volume HCl) of 100 mg of sample at ambient temperature. The calcimeter
134 was previously calibrated with pure calcite. The volume of CO₂ released during the following reaction was
135 measured with a manometer:

136



137

138

139 **XRF Ca counts**

140 High-resolution geochemical elemental composition records were measured on the archive slab core MD01-
141 2376 surface with an Avaatech XRF Core Scanner at the EPOC Laboratory (University of Bordeaux). After
142 cleaning and preparation of the surface, three separate runs (10, 30 and 50 kV, with currents of 0.6, 1.5 and 2.0
143 mA, respectively) were performed every cm down-core with a down-core slit size of 1cm. Sampling time was
144 set to 10 s at 10 kV, 15 s at 30 kV and 20 s at 50 kV. The slab surface was covered with a 4mm thick
145 SPEXCerti Prep Ultralene1 foil to avoid contamination of the XRF measurement unit and desiccation of the
146 sediment. Raw data spectra were processed by analysis of the X-ray spectra using the iterative least squares
147 software (WIN AXIL) package from Canberra Eurisys. The elements analyzed included a broad range, from
148 aluminum through uranium [32, 33]. In this paper, we only focus on calcium (Ca) results as a marker for
149 carbonates assuming the absence of other calcium rich detrital minerals.

150

151 **X-ray diffraction**

152 In this study, XRD was used to monitor the amount of calcite present in the samples at each temperature step.
153 All the samples were analyzed after thermal treatment (except for raw samples). Diffractograms provided
154 information on the mineral nature of each sample. Once calcite was identified, intensity, width at half height
155 and (1, 0, 4) peak surface were measured with MacDiff software.

156 The diffractometer used in this study was a Bruker D2 Phaser equipped with a copper anticathode (CuK α
157 radiation). Analyses were carried out according to the so-called "powders" method established by Moore &
158 Reynolds [34].

159

160 Aliquots of the three samples selected from core MD01-2376 (for both bulk and rinsed clayey hemipelagic
161 oozes) were crushed, and part of the powder (grain size less than 50 μm) was added to deionized water to form
162 mineral suspensions, that were then dispersed ultrasonically for 2 minutes. The fraction of the sediments less
163 than 2 μm in size was collected by sedimentation, and clay minerals were characterized from the XRD patterns
164 of the oriented preparations acquired in air-dried conditions, after ethylene glycol solvation and heating at 490
165 °C for 2 hours. XRD analyses were performed using a Bruker D4 Endeavor X-Ray diffractometer (CuK α
166 radiation). The oriented preparation of the fraction less than 2 μm in size was analyzed from 2° to 30° 2 θ for
167 the detailed characterization of the d₀₀₁ diffractions of phyllosilicates.

168

169 **Rock-Eval**

170 We used a Turbo Rock-Eval 6 [4]. Each individual sample was analyzed according to the Rock-Eval “Basic”
 171 cycle in which they are subjected to open pyrolysis at 300 °C to 650 °C with a 25 °C/min ramp and then to
 172 oxidation at 300 °C to 850 °C with a 20 °C/min ramp [3, 35]. Core samples were also analyzed with the method
 173 of Baudin *et al.* [2] using a pyrolysis that starts at 180 °C and a ramp of 30 °C/min.
 174 Total organic carbon (TOC) was calculated from the hydrocarbons expelled from the sample during pyrolysis
 175 as well as from the amounts of CO and CO₂ emitted during the pyrolysis and oxidation phases. The amount of
 176 mineral carbon (MinC) was calculated with Rock-Eval 6 as the sum of CO₂ released during pyrolysis, at more
 177 than 400 °C, and the CO₂ released by carbonate decomposition during oxidation, between 650 °C and 850 °C
 178 (for further explanations, see [35]).
 179

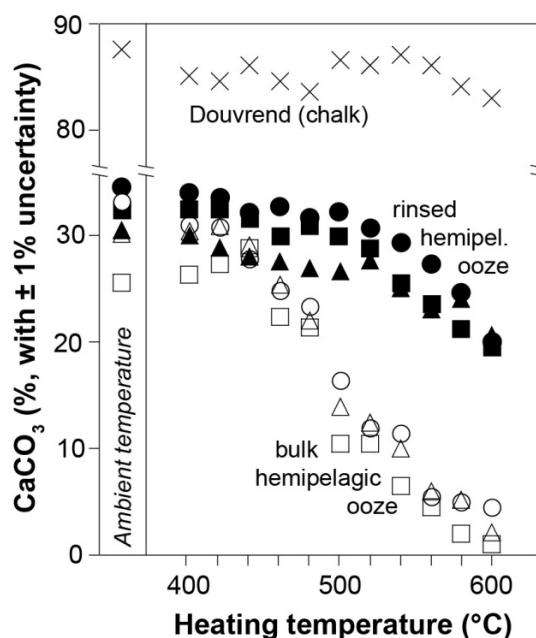
180 Scanning Electron Microscopy

181 In this study, we observed only core samples using a Zeiss Ultra 55 Field Emission Scanning Electron
 182 Microscope. Three samples corresponding to different isothermal sections for both bulk and rinsed clayey
 183 hemipelagic oozes were analyzed by SEM to characterize calcite preservation state during heating at 400 °C,
 184 480 °C and 540 °C (isothermal sections were chosen after XRD analysis to insure we focused on the
 185 temperature range of interest).
 186
 187
 188

189 2. Results and interpretations

191 2.1 Calcimetry

192
 193 The results of calcimetry during heating showed a quasi-steady state of the CaCO₃ content of the Douvrend
 194 chalk sample in the temperature range studied (loss < 5% at the final temperature) whereas the bulk clayey
 195 hemipelagic ooze samples (3 samples taken at different depths of the core) showed a marked decrease in
 196 %CaCO₃ starting at around 440 °C to reach almost 100% loss at around 600 °C (Fig. 1). However, the decrease
 197 in the rinsed clayey hemipelagic ooze samples was much less pronounced, started later (>520-540 °C) and
 198 reached a maximum of 30% loss at 600 °C. It is thus clear that rinsing the sediment influences the
 199 decomposition of CaCO₃ content with increasing temperature.
 200
 201



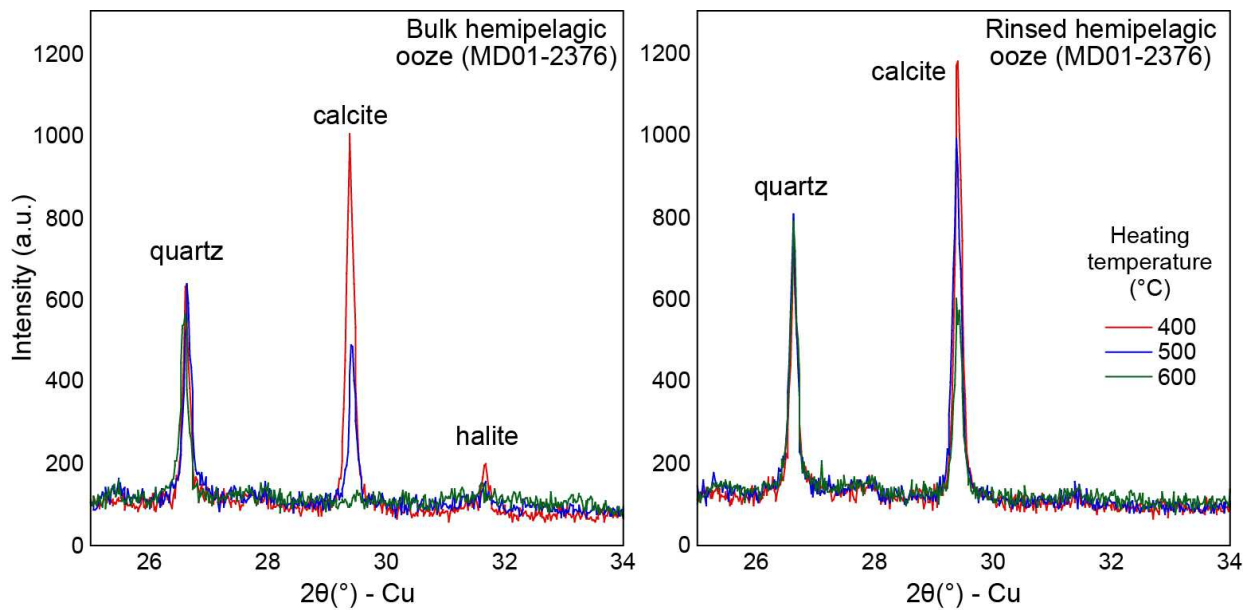
202
 203
 204 Fig. 1 – Variations in CaCO₃ content (determined using manocalcimetry) in a Cretaceous chalk indurated
 205 sample (Douvrend) and in bulk and rinsed recent clayey hemipelagic oozes from the Timor Sea, by increasing
 206 the temperature from 400 °C to 600 °C in 20 °C increments in a muffle furnace. Three samples corresponding
 207 to different core depths (triangles, squares and dots) were used for the recent clayey hemipelagic oozes from the
 208 Timor Sea.

209
210
211
212
213
214
215
216
217
218
219
220
221
222
223
224
225

2.2 X-ray diffraction

Considering the observations made with calcimetry, we thought it would be interesting to analyze the behavior of calcite and sodium chloride (NaCl), the only mineral present in the bulk hemipelagic ooze and absent in the rinsed hemipelagic ooze. The major peaks of calcite (104) and halite (200) of the bulk clayey hemipelagic ooze samples tumbled completely and synchronously between 400 °C and 600 °C (Fig. 2) whereas the intensity of the quartz peak (101) remained steady throughout the heating cycle. These diffractograms highlight the obvious relationship between the presence of salt in the samples and the early decomposition of calcite (at low temperatures) even if they do not make it possible to accurately measure the quantities.

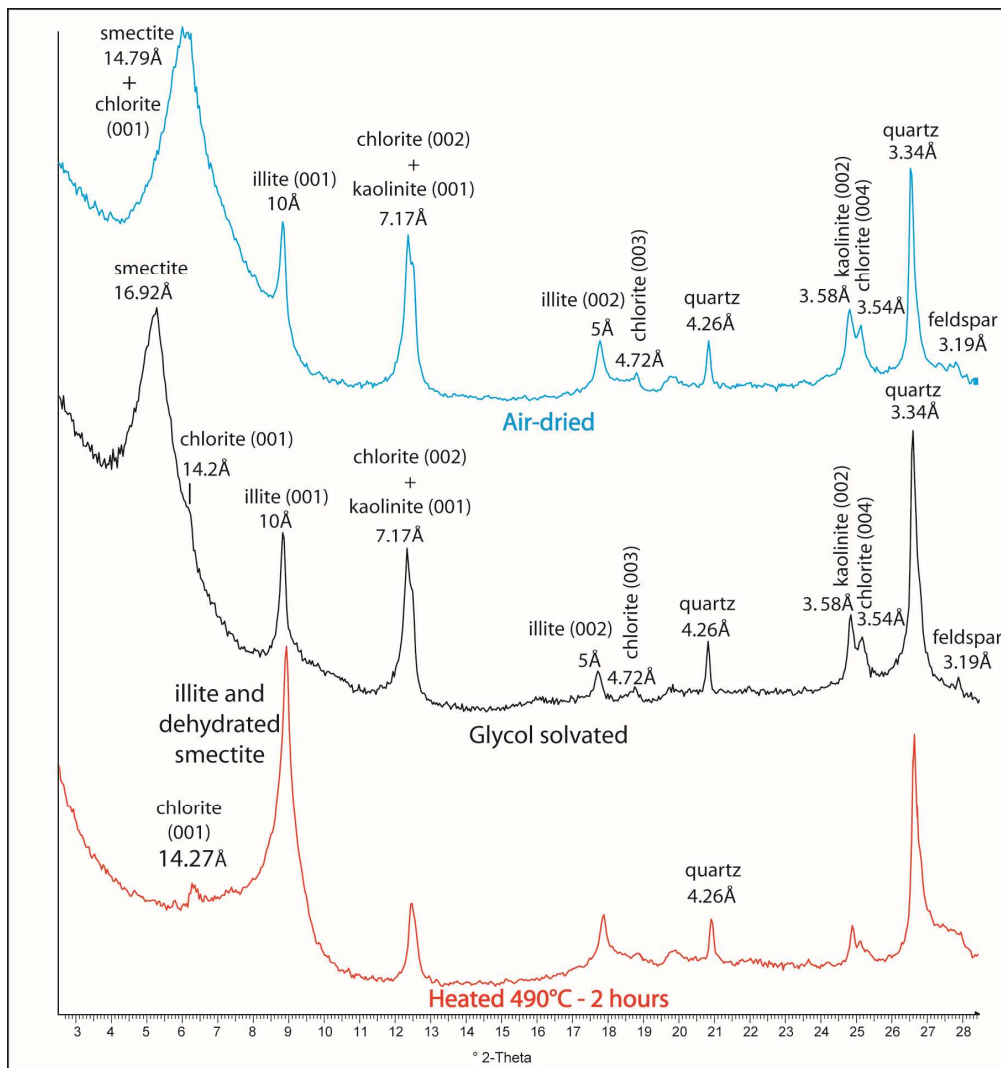
The diffractograms of the rinsed clayey hemipelagic ooze showed a slight decrease in the intensity of the calcite peak between 400 °C and 500 °C and a more significant decrease between 500 °C and 600 °C but never above 30% loss at these temperatures. Thus, when salt was removed by successive rinses and the same temperature ranges were used, the intensity of the calcite peak only decreased by half when it tumbled down to zero in the presence of salt.



226
227
228
229
230
231
232
233
234
235
236
237

Fig. 2 – Comparison of X-ray diffractograms of a bulk and rinsed clayey hemipelagic ooze from the Timor Sea at three stages of a heating experiment. Note the sharp decrease in the calcite peak (104) and in the halite peak (200) between 400 °C and 500 °C and its disappearance at 600 °C in the bulk sample. **COLOR FIGURE.**

The main components of the clay fraction of the hemipelagic ooze were of R0 type illite/smectite mixed-layers hereafter referred to as smectite (about 70%), illite (15%), chlorite (5-10%) and kaolinite (10%) (Fig. 3). Traces of R1 type illite-smectite mixed layers and chlorite-smectite mixed-layer were probably also present. Quartz and traces of feldspars equally occur in the clay fraction.



238
239

Fig. 3 X-ray diffractograms of the clay fraction of hemipelagic oozes samples in core MD01-2376.

240
241
242
243

2.3 Scanning Electron Microscopy

244

245

246

247

248

249

250

251

252

253

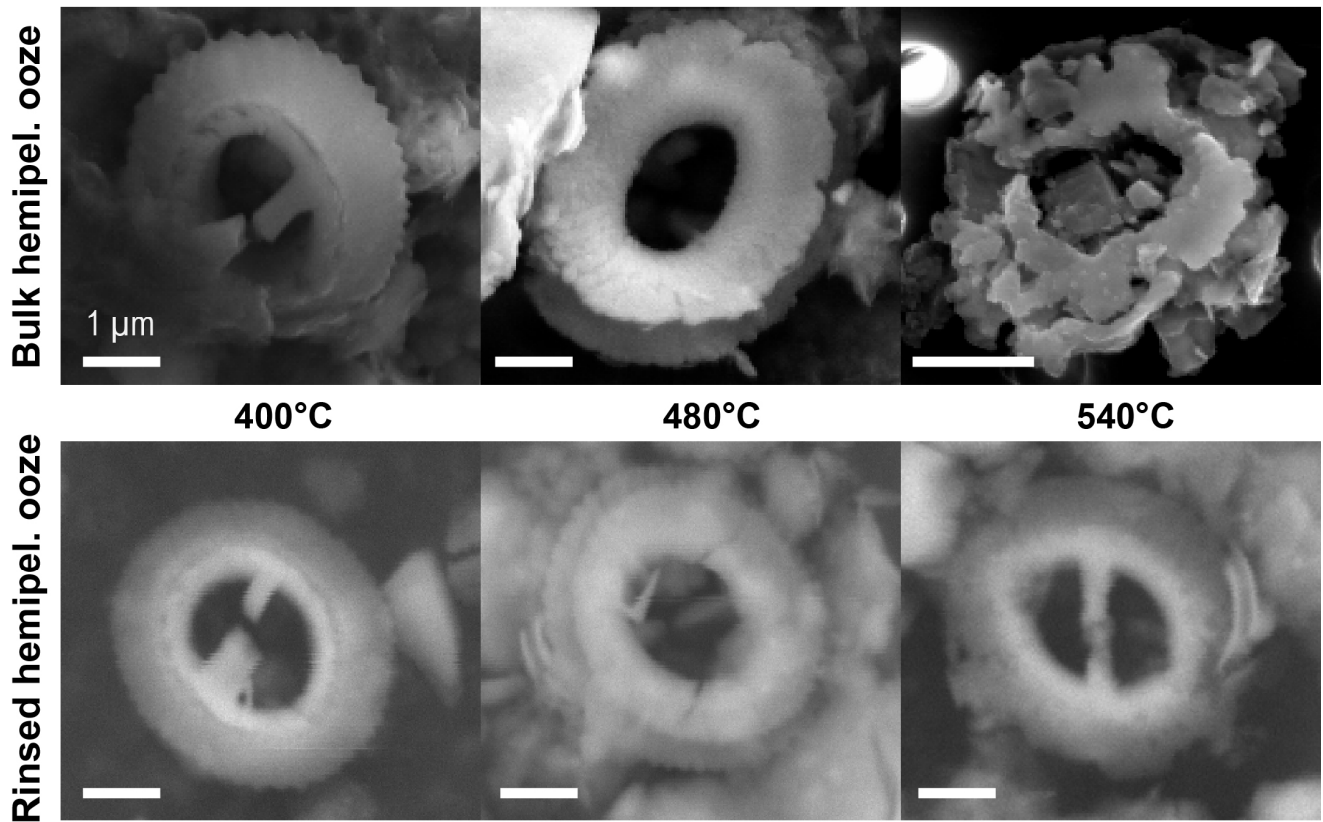
254

255

256

257

SEM observations confirmed that the carbonate fraction of clayey hemipelagic oozes was mainly composed of coccoliths and foraminifera, and subordinate micrometric calcite crystals of indeterminate origin. The coccoliths observed belong to the species *Gephyrocapsa oceanica*, characterized by a crossbar in the center of the coccolith ring. When we examined the conservation status of the nannofossil at the three temperatures previously used for the XRD on the same bulk and rinsed sediment, the differences were drastic. The bulk clayey hemipelagic ooze was subjected to severe degradation of its coccolithic content between 400 °C and 480 °C and even more at 540 °C (temperature at which it becomes almost impossible to identify the organism). Moreover, the coccolith crossbar already decomposed 480 °C. Conversely, the coccoliths in the rinsed clayey hemipelagic ooze were much better conserved with increasing temperature, the structure of the coccolith and even the crossbars were still visible at 540 °C (Fig. 4). This microscopic observation points in the same direction as the XRD results: the presence of seawater and therefore of sodium chloride is correlated with the decomposition of carbonated elements.



258
259

260 Fig. 4 – SEM images of a coccolith of the same species (*Gephyrocapsa oceanica*) at three stages (400 °C, 480
261 °C and 540 °C) of a heating experiment conducted with bulk and rinsed (desalted) powdered sediment from the
262 Timor Sea.
263

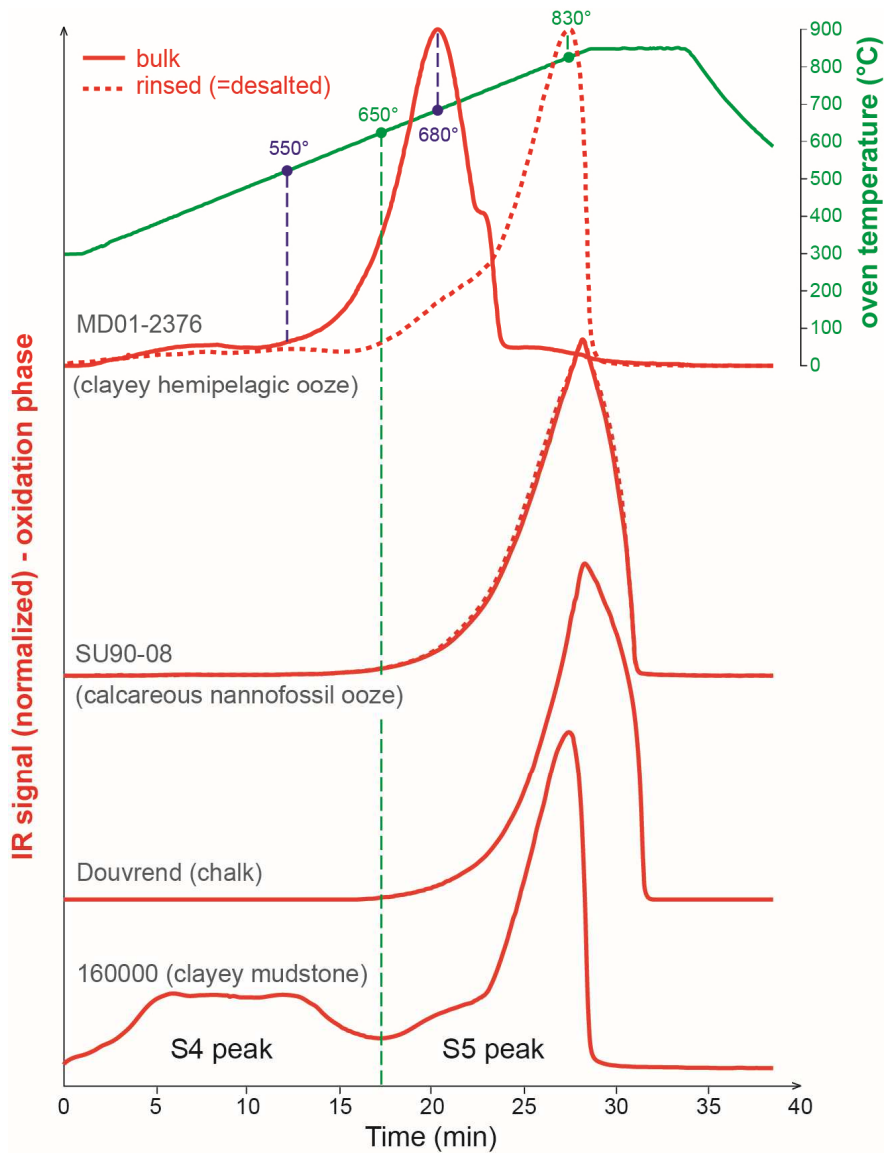
264
265

2.4 Rock-Eval

266

267 The results of Rock-Eval in this study highlight the difference in the behavior of sediments components
268 subjected to heating cycles. Looking at the CO₂ curves corresponding to decomposition of carbonates during
269 the oxidation step (the so-called S5 peak) we observed two clearly different behaviors. Decomposition of the
270 calcite in the fossil sediment samples Douvrend and IFP160000 (used as Rock-Eval standard) started at around
271 650 °C and reached zero around 830 °C, as also demonstrated by Pillot *et al.* [1]. The nannofossil pelagic ooze
272 (SU90-08) had almost exactly the same CO₂ signature whether it was rinsed or not. The S5 peak of all the
273 samples showed very similar shapes. On the other hand, our results revealed a disparity between the bulk and
274 the rinsed clayey hemipelagic ooze. While the rinsed sample signal was almost identical to those discussed
275 previously, the bulk signal shifted on the temperature scale. In the bulk clayey hemipelagic ooze, carbonate
276 decomposition started early at around 400 °C increased at around 550 °C and peaked at 680 °C (Fig. 5).

276



277
278

279 Fig. 5 – Infrared CO₂ cell-detector response (corresponding to the S4CO₂ and S5 peaks of Rock-Eval) for two
280 recent sediment samples, one from the Timor Sea (clayey hemipelagic ooze/MD01-2376, ~30% CaCO₃) and
281 the other from the central Atlantic Ocean (nannofossil pelagic ooze/SU90-08, ~90% CaCO₃). Each sample was
282 analyzed before (as bulk sediment, solid line) and after rinsing (desalted sediment, dashed line). The S4CO₂ and
283 S5 peaks for the chalk sample (Douvrend) and the IFP 160000 are shown for the sake of comparison. **COLOR**
284 **FIGURE.**

285

286

287

288

3. Discussion

289

290

291

When a sediment or a sedimentary rock is heated, several modifications take place and are accompanied by mass loss. The loss of mass may be due to the moisture in the sample, the presence of structural water or hydroxide (OH⁻) anions in minerals such as clays, destruction of both organic and mineral phases, etc.

292

293

294

The organic phase is often the first to be destroyed, followed by the decomposition and/or the neof ormation of mineral phases. This study focused on identifying the factors responsible for the early thermal destruction of carbonates.

295

296

297

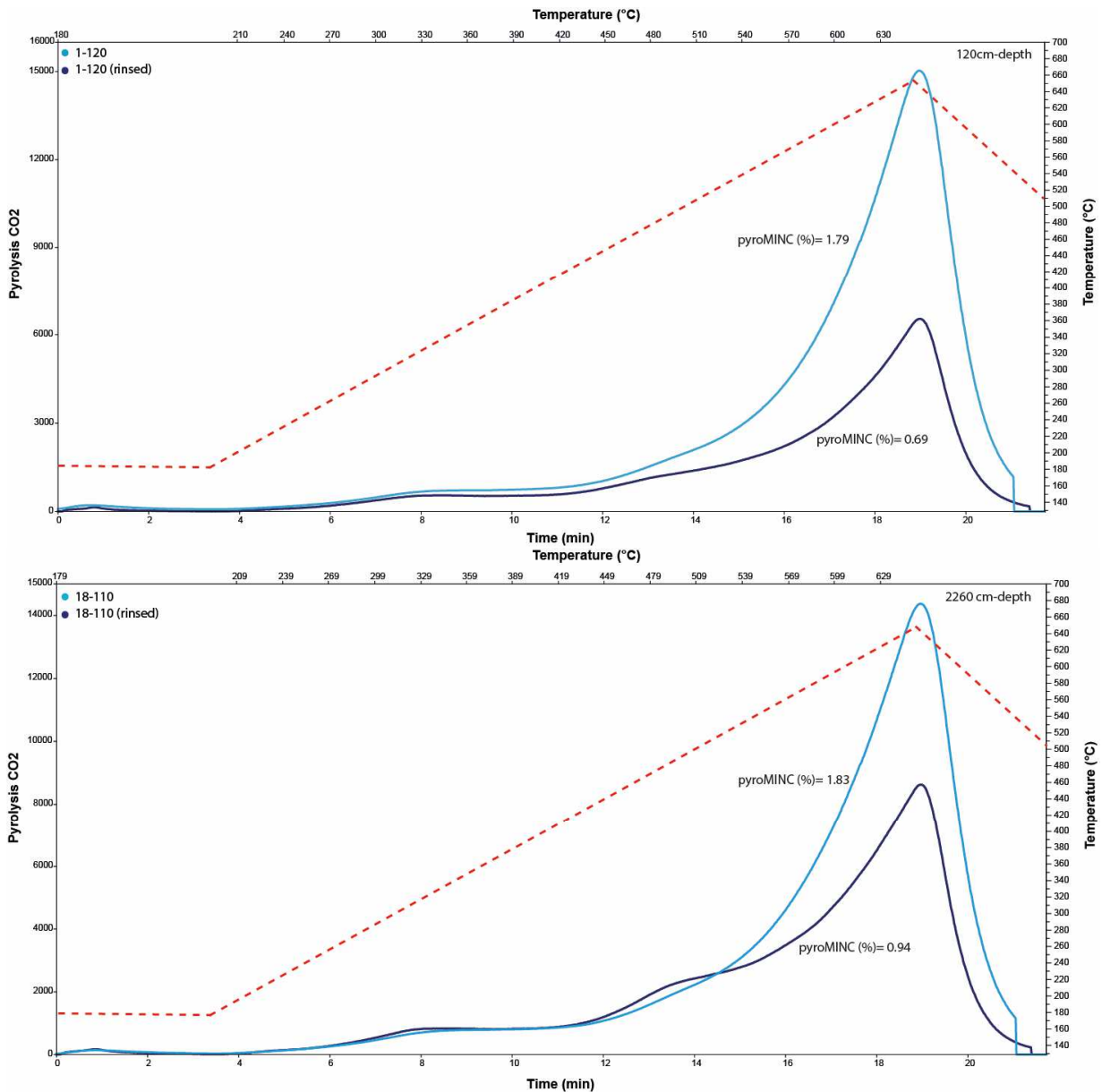
298

This study highlight the relationship between the presence of salt (NaCl) in the samples and the early decomposition of calcite. Therefore, the hypothesis we proposed in a previous study [2] according to which the thermally labile character of poorly crystallized minerals in recent sediments are responsible for the early decomposition of carbonates is not validated. This study revealed different calcite decomposition behaviors in

299 two different recent sediments: a nannofossil pelagic ooze and a clayey hemipelagic ooze (Fig. 5). Calcite
300 decomposition in the nannofossil pelagic ooze occurred in the same temperature ranges as fossil sediments such
301 as Douvrend (chalk) and IFP16000, whether bulk or rinsed. On the other hand, the bulk clayey hemipelagic
302 ooze calcite decomposed at lower temperatures although with a similar curve shape. This observation led us to
303 the crucial identification of the cause of these different behaviors, i.e. the presence or absence of clays and
304 hence of structural water and hydroxyl groups in the sediment.

305 The other methods of analysis used in this study confirmed the responsibility not only of the presence of salt in
306 the sediments but particularly the water and/or hydroxide anions in the early stage of decomposition of the
307 carbonates. XRD analysis (Fig. 2) showed that in the rinsed clayey hemipelagic ooze, the decomposition of
308 calcite is not early even if a small amount of salt remains in the sample. However a small reduction in the
309 calcite principal peak (104) intensity at 600 °C was observed corresponding the classical thermal
310 decomposition ranges of this mineral [1]. On the other hand, the bulk clayey hemipelagic ooze calcite started
311 decomposing between 400 °C and 500 °C and was already absent from the sample at 600 °C. These
312 observations were visually confirmed by SEM and calcimetry analyses (respectively Fig. 4 and 1). According
313 to the results of calcimetry based on the samples heated in the muffle furnace, the calcite content of the fossil
314 sample (Douvrend) and rinsed clayey hemipelagic ooze started decreasing around 550 °C (in agreement with
315 the onset reported by Pillot *et al.* [1]), whereas in the bulk clayey hemipelagic ooze, carbonate content reached
316 almost zero at the same temperature. When the sample was rinsed and dried the water present in it evaporated.
317 It is therefore the presence of water and/or hydroxide anions combined with chloride salt in our samples that
318 triggered the early decomposition of carbonates.

319 It is also interesting to note the difference between the temperature of calcite decomposition in the bulk clayey
320 hemipelagic ooze sample between calcimetry (around 450 °C) and the Rock-Eval oxidation cycle (starting
321 around 450 °C but only becoming significant at around 550 °C). This shift in carbonate decomposition
322 temperatures can be simply explained by the pyrolysis phase undergone before oxidation during the Rock-Eval
323 analysis. Considering this cycle brings the sample up to a temperature of 650 °C (Fig. 6), unlike the calcimetry
324 and SEM post thermal protocol analyses, some of the carbonates have already been attacked during pyrolysis.
325 Rock-Eval analyses of rinsed clayey hemipelagic ooze confirmed this observation by showing lower mineral
326 CO₂ values during pyrolysis and standard degradation of calcite in chalk-like temperature ranges. Moreover,
327 the difference in pyroMINC values between rinsed and bulk samples decreased in accordance with the depth of
328 the sample (factor of about 2.5 between pyroMINC values for a sample located at 120cm from the top of the
329 core versus 2 for a deeper sample located at 2260cm from the top of the core), which is to be expected since the
330 sediments contain progressively less water and salt with compaction due to the depth.



331

332

333

334

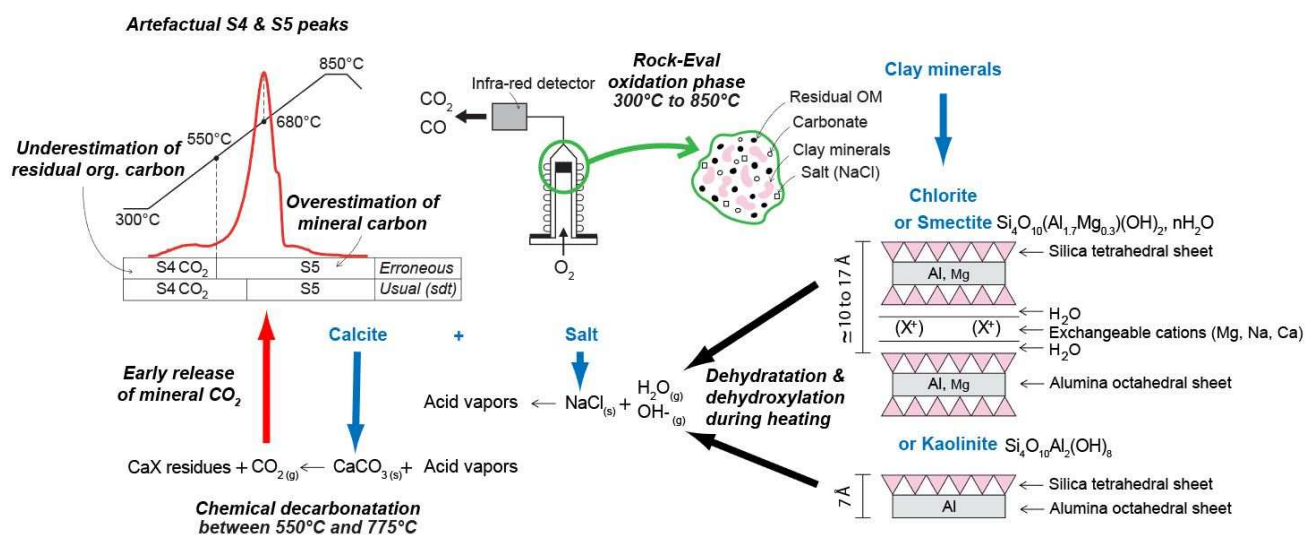
335 Fig. 6 – Pyrograms of two core samples (at 120 cm and 2260 cm-depth respectively) highlighting the onset of
 336 decomposition of carbonates in bulk sediments during Rock-Eval pyrolysis. **COLOR FIGURE.**

337

338

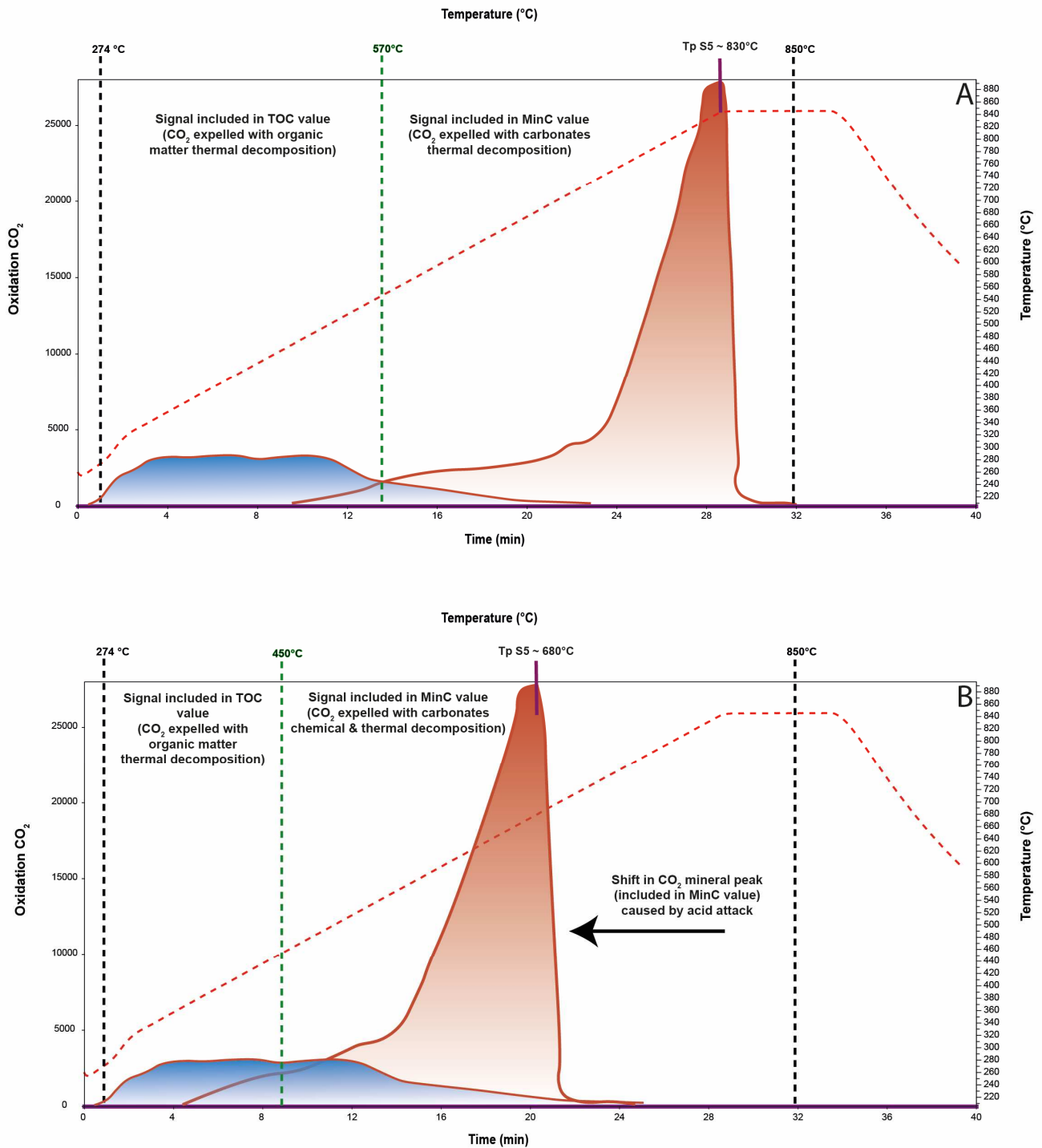
339 The phenomenon of early decomposition of carbonates in some recent sediments can be explained as follows.
 340 The clays have a layered structure that can contain water. Clay minerals consist of silicon, aluminum, oxygen
 341 and hydroxyl (OH) ions, organized in layers of two types depending on whether the oxygen atoms or hydroxyl
 342 groups are associated in tetrahedra or octahedra. The octahedral and tetrahedral layers coalesce along planes,
 343 pooling O and OH, so the sheets are separated by interfoliar spaces. Positive charge deficit can occur due to
 344 possible partial substitutions of Si^{4+} by Al^{3+} in the tetrahedra, Al^{3+} by Mg^{2+} , Fe^{2+} or Fe^{3+} , in the octahedra. This
 345 is then offset by the insertion of cations or water in the interfoliar spaces. Water molecules are in fact no longer
 346 present in the structure but have been expelled as a result of thermal decomposition [36]. When a sediment
 347 containing clay minerals is heated, dehydration takes place around 100 °C, releasing water from the clay
 348 interlayers. Given the fact that the clay fraction of hemipelagic oozes consists mainly of smectites (Fig. 3),
 349 dehydration had to provide a significant amount of water vapor. At higher temperatures around 500 °C,
 350 depending on the nature of the clay minerals, dehydroxylation occurs [37, 38, 39, 40, 41, 42] Moreover Du et
 351 al. [43] measured melting temperature of chloride salt (NaCl) at 420 °C. These temperatures coincide perfectly
 352 with the early decomposition temperatures of calcite observed in our experiments.

353 Dehydroxylation is significant notably in chlorite and kaolinite, two clay minerals that occur in significant
 354 quantities in the samples of hemipelagic oozes collected from the Timor Sea and analysed in the present study.
 355 Consequently, and when salted pore water is also present in the sediment, released gaseous water (H₂O) and/or
 356 hydroxide anions react with it to form acid vapor (such as hypochlorous acid (HClO) or hydrochloric acid
 357 (HCl)). In turn, this acid vapor, reacts with the carbonates (CaCO₃) present in the sediment causing chemical
 358 decarbonation, which manifests itself as the release of CO₂. In this case, the phenomenon of carbonate
 359 destruction is therefore chemical and non-thermal, giving rise to early release of CO₂ and hence to artificial
 360 peaks during Rock-Eval analysis. The CO₂ peak corresponding to the destruction of the carbonate phase of the
 361 sediment (S5) thus shifts on the temperature scale, leading to overestimation of mineral carbon and
 362 underestimation of organic carbon (Fig. 7).
 363



364
 365
 366
 367
 368 Fig. 7 – Plausible origin of the artefactual S5 peak that appears during Rock-Eval analysis (oxidation phase) of
 369 recent marine sediment containing hydrated clay minerals, salt and carbonates. An acid reaction between NaCl
 370 and water provided by the dehydration/dihydroxylation of clay minerals causes the dissolution of calcite,
 371 with the resulting generation of CO₂ at temperatures ranging between 550 °C and 775 °C. **COLOR FIGURE.**
 372

373 However, it is important to really understand the shift of this oxidation CO₂ peak. It would be easy to think that
 374 the entire peak of CO₂ shifts which would lead to a reverse observation, i.e. an overestimation of the TOC and
 375 underestimation of the MinC since part of the peak associated with the mineral carbon would be included in
 376 signal integrated as organic carbon. It is in fact only the mineral part of the oxidation CO₂ peak which is
 377 shifted, the formation of acid vapors having no influence on the decomposition temperatures of the organic
 378 carbon. Thus, when the mineral part of the CO₂ peak shifts to lower temperatures, the Rock-Eval cursor
 379 defining the boundary between the portions of the curve integrated as organic and the one integrated as mineral
 380 seeks a new minimum on the curve (Fig. 8). As this minimum is most often located at much lower
 381 temperatures, the software integrates a large part of the organic signal as mineral carbon against a small part of
 382 the mineral signal as an organic carbon thus explaining the phenomenon of overestimation/underestimation
 383 observed.



384
385

386

387 Fig. 8 – Illustration of the position of the cursor separating the organic carbon from the mineral carbon on the
388 CO₂ signal in oxidation for a classical analysis (A) versus an analysis showing the shift of the mineral part of
389 the CO₂ (B) following an early decomposition of the carbonates by chemical attack. **COLOR FIGURE.**

390

391

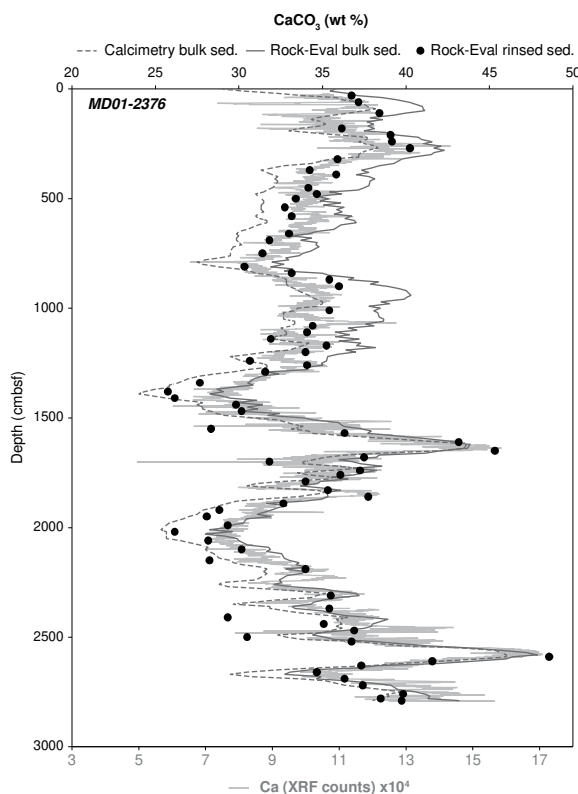
392

393 **4. Application**
394 An example of application is presented below to highlight the importance of rinsing recent carbonate sediment
395 samples before analysis. Figure 9 shows four curves representing the percentage of CaCO₃ obtained with
396 different methods (calcimetry, Rock-Eval, XRD and XRF) along a core of hemipelagic sediments collected
397 from the Timor Sea. The curve obtained with XRF analyses (light grey line) is a reference curve, since it is not
influenced by any other factors than the carbonate content.

398 Rock-Eval analyses of the bulk sediment (solid line) overestimate carbonate contents while those obtained
 399 using calcimetry (dotted line) underestimate them. Indeed, as seen above, the presence of water in the clays and
 400 salt in the sediment causes early chemical degradation of the carbonates during the Rock-Eval analysis,
 401 inducing a shift of the CO₂ peak emitted and hence overestimation of mineral carbon. When calcimetry is used,
 402 this phenomenon does not occur because the sample is not heated. However with calcimetry, there is also an
 403 error in the estimation of the percentage of CaCO₃. Indeed, the presence of salt in the sample during weighing
 404 results in overestimation of the weight of the sample and hence to an underestimation of the carbonate content.
 405 During Rock-Eval of the rinsed sediments, the analyzed sample no longer contains salt, and its carbonate
 406 contents are consequently much closer to those obtained with XRF (black dots). This observation confirms the
 407 results of our study and highlights the importance of using properly processed samples before analysis and
 408 interpretation of the results.

409
 410 It is also interesting to note the variation in these shifts between the different methods and along the core. We
 411 observed indeed that the gap between the CaCO₃ percentages produced by Rock-Eval for the bulk sediment and
 412 the XRF analyses is much larger in the top part of the core but narrows towards the deeper part. This
 413 observation can be explained by simple geological phenomena. Indeed, the upper part of the core (close to the
 414 surface) is comprised of highly porous sediments and consequently contain a lot of interstitial marine water,
 415 resulting in a large quantity of salt when the sediment is oven dried. Towards the deeper parts, when
 416 compaction takes effect, the porosity of the sediment decreases and consequently contains less water and fewer
 417 salt crystals after drying, thereby limiting errors caused by their presence.

418



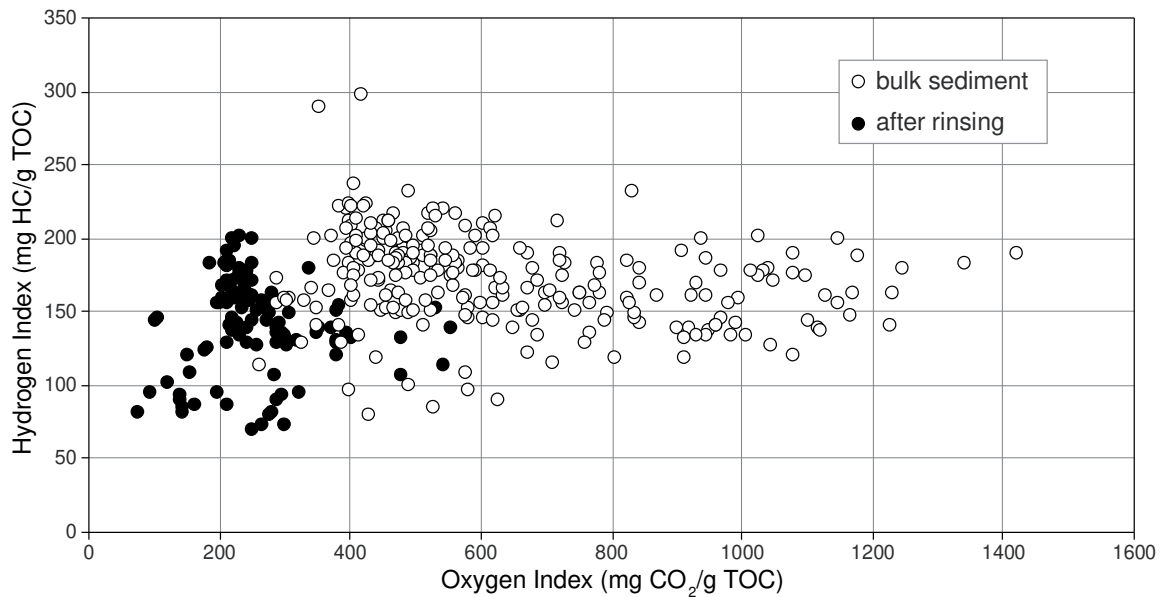
419
 420

421 Fig. 9 – Changes (5 point-smoothing) in CaCO₃ contents along a 27.9 m-long core of hemipelagic sediments
 422 from the Timor Sea. The data were acquired using a calcimetric bomb (dotted line) or were derived from the
 423 MinC of Rock-Eval (solid line) of the bulk sediment. Selected samples were rinsed using deionized water and
 424 re-analyzed using Rock-Eval (black dots). Variations in the Ca content (light grey line) derived from XRF are
 425 shown for the sake of comparison. The latter are in good agreement with CaCO₃ determined in rinsed
 426 sediments.

427
 428

429 Beyond overestimation of mineral carbon and underestimation of organic carbon, the analysis of recent bulk
 430 sediments may lead to other misinterpretations. In fact, a certain number of parameters such as the oxygen
 431 index (OI) used to define the origin of organic matter are calculated from the CO₂ emission curves obtained
 432 during the Rock-Eval analysis. Thus, if this analysis is distorted by a phenomenon such as the early destruction

433 of carbonates through a chemical reaction, the CO₂ emission curves shift and the parameters based on them are
434 no longer reliable. This is highlighted in figure 10 below, where the OI reaches 1400mg CO₂/g TOC for bulk
435 sediment whereas it does not exceed 600 in the rinsed sediment, a drastic difference for an interpretation based
436 on the pseudo van Krevelen diagram, for example.
437



438
439

440 Fig. 10 – Comparison of organic matter typing using a modified van Krevelen diagram (HI-OI) for bulk and
441 rinsed samples of recent hemipelagic sediment from the Timor Sea. The extremely high OI values for bulk
442 sediment are artefactual (see Fig. 5 for explanation).
443

444

445 Finally, an important point when comparing bulk and rinsed sediments that has not yet been discussed in this
446 paper is the mass effect. Indeed, the weight of a bulk sample is not the same as that of a rinsed sample because
447 the salt disappears along with part (soluble) of the organic carbon. This effect must of course be taken into
448 account but accounts for a minimum part of the observed differences between the bulk and rinsed samples.
449 Figure 8 shows that the OI of the average bulk samples is around 600 mg CO₂/g TOC versus 300mg CO₂/g
450 TOC for rinsed samples. If the cause of this very large difference was only linked to the loss of mass, this
451 would imply a factor of 2 between TOC values of the bulk and rinsed samples. However it is very unlikely that
452 rinsing causes such a difference in TOC between the bulk and the rinsed sample, let alone that the mass loss
453 due to the removing of salt and the loss of part of the organic carbon is entirely responsible for such a
454 difference. Moreover, core analyses allow us to definitely disregard the impact of this phenomenon in this
455 study. Indeed, the TOC of sample 1-120 (120 cm from the top of the core) was 0.6% for the bulk sample versus
456 1.15 for the rinsed sample. This result confirms the underestimation of organic carbon discussed previously in
457 this article but also make it possible to hold the mass effect responsible for this difference. However, sample
458 18-110 (taken deeper in the core at 2260 cm) was much more compacted than sample 1-120 and therefore did
459 not contain enough water to cause the early chemical dissolution reaction of the carbonates. The TOC values
460 for the rinsed and non-rinsed samples were almost identical (~ 1.11%), thereby confirming the negligible effect
461 of mass loss in this situation.
462

463

463 Conclusion

464

465 Rock-Eval analyzes, widely used in the oil industry, were recently found to be appropriate for inferring the
466 CaCO₃ content of a sample and identifying the type of carbonates it contains [1]. However, the relevance of the
467 CO₂ production curve shape and temperature ranges obtained during thermal destabilization of carbonates is
468 called into question by the transposition of this method to recent clayey sediments. Indeed, calcite (and
469 probably all carbonates in recent sediments) becomes unstable at temperatures much lower than those of the
470 fossil sedimentary rocks on which the mineral recognition records in the literature are based. Our study allowed
471 us to highlight a shift in peak CO₂ temperatures observed with Rock-Eval and corresponding to the destruction
472 of the carbonate phase within a sediment. This phenomenon is due to the combined presence of salt and water

473 and/or hydroxide anions expelled from clay minerals that leads to an acid reaction and early decomposition of
474 carbonates itself leading to overestimation of mineral carbon and underestimation of organic carbon. Moreover,
475 this CO₂ curve can also be misinterpreted if one relies on the CO₂ peaks obtained with Rock-Eval to identify
476 the type of carbonate present in the sample according to the method of Pillot *et al.* [1]. The same goes for the
477 OI that is overestimated due to underestimation of organic carbon. Care should thus be taken when analyzing
478 recent hemipelagic samples and the samples should be thoroughly rinsed before analysis and interpretation to
479 avoid any misinterpretation of the results.

480

481 **Acknowledgments**

482

483 The authors would like to thank F. Minoletti (Sorbonne Université), F. Bassinot (LSCE, chief scientist
484 WEPEMA cruise) and E. Moreno (curator of the marine core repository at French National Museum of Natural
485 History) for providing necessary samples for the study. W. Liu is acknowledged for the CaCO₃ measurements
486 made on core MD01-2376 during his PhD thesis. We are indebted to F. Savignac and O. Boudouma, technical
487 staff of the equipment used. Finally, we acknowledge the editor of JAAP and an anonymous reviewer for their
488 comments on an earlier draft of this paper.

489

490

491 This research did not receive any specific grant from funding agencies in the public, commercial, or not-to-
492 profit sectors.

- 495 [1] Pillot D., Deville E., Prinzhofer A. (2014) Identification and Quantification of Carbonate Species Using
496 Rock-Eval Pyrolysis, *Oil & Gas Sci. Technol.*, **69**, 341-349. <https://doi.org/10.2516/ogst/2012036>.
- 497 [2] Baudin F., Disnar J.R., Aboussou A., Savignac F. (2015) Guidelines for Rock-Eval analysis of recent
498 marine sediments, *Organic Geochemistry*, **86**, 71-80. <http://dx.doi.org/10.1016/j.orggeochem.2015.06.009>.
- 499 [3] Espitalié J., Marquis F., Sage L. (1986) La pyrolyse Rock-Eval et ses applications, *Revue de l'institut*
500 *Français du Pétrole*, **41**, 73-89. <https://doi.org/10.2516/ogst:1986003>.
- 501 [4] Lafargue E., Marquis F., Pillot D. (1998) Rock-Eval 6 applications in hydrocarbon exploration, production,
502 and soil contamination studies, *Oil & Gas Sci. Technol.*, **53**, 421-437. <https://doi.org/10.2516/ogst:1998036>.
- 503 [5] Peters K.E., Simoneit B.R.T. (1982) Rock-Eval pyrolysis of Quaternary sediments from leg-64, site 479
504 and site 480, Gulf of California, *Initial Reports of the Deep Sea Drilling Project*, **64**, 925-931.
505 <https://doi.org/10.2973/dsdp.proc.64.138.1982>.
- 506 [6] Di Giovanni C., Disnar J.R., Bichet V., Campy M. and Guillet B. (1998) Geochemical characterization of
507 soil organic matter and variability of a postglacial detrital organic supply (Chaillexon Lake, France), *Earth*
508 *Surface Processes and Landforms*, **23**, 1057-1069. [https://doi.org/10.1002/\(SICI\)1096-9837\(199812\)23:12<1057::AID-ESP921>3.0.CO;2-H](https://doi.org/10.1002/(SICI)1096-9837(199812)23:12<1057::AID-ESP921>3.0.CO;2-H).
- 510 [7] Jacob J., Disnar J.R., Boussafir M., Sifeddine A., Turcq, B., Albuquerque A.L.S. (2004) Major
511 environmental changes recorded by lacustrine sedimentary organic matter since the last glacial maximum near
512 the equator (Lagoa do Caco, NE Brazil), *Palaeogeography, Palaeoclimatology, Palaeoecology*, **205**, 183-
513 197. <https://doi.org/10.1016/j.palaeo.2003.12.005>.
- 514 [8] Sanei H., Stasiuk L.D., Goodarzi F. (2005) Petrological changes occurring in organic matter from recent
515 lacustrine sediments during thermal alteration by Rock-Eval pyrolysis, *Organic Geochemistry*, **36**, 1190-1203.
516 <https://doi.org/10.1016/j.orggeochem.2005.02.009>.
- 517 [9] Baudin F., Combourieu-Nebout, N., Zahn, R. (2007) Organic signatures of rapid climatic changes in
518 Western Mediterranean during North Atlantic cold events of the Last Glacial. *Bulletin de la Société Géologique*
519 *de France*, **178**, 3-13. <http://dx.doi.org/10.2113/gssgfbull.178.1.3>.
- 520 [10] Kim J.H., Park M.H., Tsunogai U., Cheong T.J., Ryu B.J., Lee Y.J., Han H.C., Oh J.H., Chang H.W.
521 (2007) Geochemical characterization of the organic matter, pore water constituents and shallow methane gas in
522 the eastern part of the Ulleung Basin, East Sea (Japan Sea), *Island Arc*, **16**, 93-104.
523 <https://doi.org/10.1111/j.1440-1738.2007.00560.x>.
- 524 [11] Marchand C., Lallier-Vergès E., Disnar J.R., Kéravis D. (2008) Organic carbon sources and
525 transformations in mangrove sediments: a Rock-Eval pyrolysis approach, *Organic Geochemistry*, **39**, 408-421.
526 <https://doi.org/10.1016/j.orggeochem.2008.01.018>.
- 527 [12] Tribouvillard N., Bout-Roumazelles V., Algeo T., Lyons T.W., Sionneau T., Montero-Serrano J.C.,
528 Riboulleau A., Baudin F. (2008) Paleodepositional conditions in the Orca Basin as inferred from organic matter
529 and trace metal contents, *Marine Geology*, **254**, 62-78. <https://doi.org/10.1016/j.margeo.2008.04.016>.
- 530 [13] Biscara L., Mulder T., Martinez P., Baudin F., Etcheber H., Jouanneau J.M., Garlan T. (2011) Transport of
531 terrestrial organic matter in the Ogooué deep sea turbidite system (Gabon), *Marine and Petroleum Geology*, **28**,
532 1061-1072. <https://doi.org/10.1016/j.marpetgeo.2010.12.002>.
- 533 [14] Riboulleau A., Tribouvillard N., Baudin F., Bout-Roumazelles V., Lyons T. (2011) Unexpectedly low
534 organic matter content in Cariaco Basin sediments during the Younger Dryas: origin and implications, *Comptes*
535 *Rendus Geosciences*, **343**, 351-359. <https://doi.org/10.1016/j.crte.2011.04.001>.
- 536 [15] Boussafir M., Sifeddine A., Jacob J., Foudi M., Cordeiro R.C., Albuquerque A.L.S., Abrao J.J., Turcq B.
537 (2012) Petrographical and geochemical study of modern lacustrine sedimentary organic matter (Lagoa do Caco,
538 Maranao, Brazil): relationship between early diagenesis, organic sedimentation and lacustrine filling, *Organic*
539 *Geochemistry*, **47**, 88-98. <https://doi.org/10.1016/j.orggeochem.2012.03.013>.
- 540 [16] Zocatelli R., Turcq B., Boussafir M., Cordeiro R.C., Disnar J.R., Costa R.L., Sifeddine A.,
541 Albuquerque A.L.S., Bernardes M.C., Jacob J. (2012) Late Holocene paleoenvironmental changes in
542 Northeast Brazil recorded by organic matter in lacustrine sediments of Lake Boqueirão.
543 *Palaeogeography, Palaeoclimatology, Palaeoecology*, **363**, 127-134.
544 <https://doi.org/10.1016/j.palaeo.2012.08.021>
- 545 [17] Lavrieux M., Disnar J.R., Chapron E., Bréhéret J.G., Jacob J., Miras Y., Reyss J.L., Andrieu-Ponel V.,
546 Arnaud F. (2013) A 6700 yr sedimentary record of climatic and anthropogenic signals in Lake Aydat (French
547 Massif Central), *Holocene*, **23**, 1317-1328. <https://doi.org/10.1177/0959683613484616>.

- 548 [18] Hare A.A., Kuzyk Z.Z.A., Macdonald R.W., Sanei H., Barber D., Stern G.A., Wang F.Y. (2014)
549 Characterization of sedimentary organic matter in recent marine sediments from Hudson Bay, Canada, by
550 Rock–Eval pyrolysis, *Organic Geochemistry*, **68**, 52–60. <https://doi.org/10.1016/j.orggeochem.2014.01.007>.
- 551 [19] Hatcher P., Ravin A., Behar F., Baudin F. (2014) Diagenesis of organic matter in a 400m organic rich
552 sediment core from offshore Namibia using solid state ¹³C NMR and FTIR, *Organic Geochemistry*, **75**, 8–23.
553 <https://doi.org/10.1016/j.orggeochem.2014.05.016>.
- 554 [20] Deville E., Mascle A., Callec Y., Huyghe P., Lallemand S., Lerat O., Mathieu X., Padron de Carillo C.,
555 Partiat M., Pichot T., Loubrieux B., Granjeon D. (2015) Tectonics and sedimentation interactions in the east
556 Caribbean subduction zone: An overview from the Orinoco delta and the Barbados accretionary prism. *Marine
557 and Petroleum Geology*, **64**, 76–103. <https://doi.org/10.1016/j.marpetgeo.2014.12.015>.
- 558 [21] Disnar J.R., Guillet B., Keravis D., Di Giovanni C. and Sebag D. (2003) Soil organic matter (SOM)
559 characterization by Rock–Eval pyrolysis: scope and limitations, *Organic Geochemistry*, **34**, 327–343.
560 [https://doi.org/10.1016/S0146-6380\(02\)00239-5](https://doi.org/10.1016/S0146-6380(02)00239-5)
- 561 [22] Hetényi M., Nyilas T. (2014) Soil organic matter characterization using S3 and S4 signals from Rock–Eval
562 pyrolysis, *Pedosphere*, **24**, 563–574. [https://doi.org/10.1016/S1002-0160\(14\)60042-4](https://doi.org/10.1016/S1002-0160(14)60042-4).
- 563 [23] Sebag D., Disnar J.R., Guillet B., Di Giovanni C., Verrecchia E.P., Durand A. (2006) Monitoring organic
564 matter dynamics in soil profiles by ‘Rock–Eval pyrolysis’: bulk characterization and quantification of
565 degradation, *European Journal of Soil Science*, **57**, 344–355. [https://doi.org/10.1111/j.1365-
566 2389.2005.00745.x](https://doi.org/10.1111/j.1365-2389.2005.00745.x).
- 567 [24] Saenger A., Cecillon L., Sebag D., Brun J.J. (2013) Soil organic carbon quantity, chemistry and thermal
568 stability in a mountainous landscape: a Rock–Eval pyrolysis survey, *Organic Geochemistry*, **54**, 101–114.
569 <https://doi.org/10.1016/j.orggeochem.2012.10.008>.
- 570 [25] Hetényi M., Nyilas T., Toth, T.M. (2005) Stepwise Rock–Eval pyrolysis as a tool for typing heterogeneous
571 organic matter in soils, *Journal of Analytical and Applied Pyrolysis*, **74**, 45–54.
572 <https://doi.org/10.1016/j.jaap.2004.11.012>.
- 573 [26] Barré P., Plante A.F., Cécillon L., Lutfalla S., Baudin F., Bernard S., Christensen B.T., Eglin T.,
574 Fernandez J.M., Houot S., Kätterer T., Le Guillou C., McDonald A., Van Oort F., Chenu C. (2016) The
575 energetic and chemical signatures of persistent soil organic matter, *Biogeochemistry*, **130**, 1–12.
576 <https://doi.org/10.1007/s10533-016-0246-0>.
- 577 [27] Soucémariadin L., Cécillon L., Chenu C., Baudin F., Nicolas M., Girardin C., Barré P. (2018) Is Rock-
578 Eval 6 thermal analysis a good indicator of soil organic carbon lability? A method-comparison study in forest
579 soils, *Soil Biology and Biochemistry*, **117**, 108–116. <https://doi.org/10.1016/j.soilbio.2017.10.025>.
- 580 [28] Ferré B. (1995) Incidence des événements anoxiques océaniques sur les microfaunes Cénomano-
581 Turoniennes du bassin Anglo-Parisien, *PhD Thesis*, Pierre et Marie Curie University, Paris, 213–223.
- 582 [29] Liu W., Baudin F., Moreno E., Dewilde D., Caillon N., Fang N., Bassinot F. (2014) Comparison of 240ka
583 long organic carbon and carbonate records along a depth transect in the Timor Sea: Primary signals versus
584 preservation changes, *Paleoceanography*, **29**, 389–402. <https://doi.org/10.1002/2013PA002539>.
- 585 [30] Vidal L., Labeyrie L., Cortijo E., Arnold M., Duplessy J.C., Michel E., Becque S., Van Weering T. (1997)
586 Evidence for changes in the North Atlantic Deep Water linked to meltwater surges during the Heinrich events,
587 *Earth Planet. Sci. Lett.*, **146**, 13–27. [https://doi.org/10.1016/S0012-821X\(96\)00192-6](https://doi.org/10.1016/S0012-821X(96)00192-6).
- 588 [31] Candelier Y., Minoletti F., Probert I., Hermoso M. (2013) Temperature dependence of oxygen
589 isotope fractionation in coccolith calcite: A culture and core top calibration of the genus *Calcidiscus*.
590 *Geochimica et Cosmochimica Acta*, **100**, 264–281. <https://doi.org/10.1016/j.gca.2012.09.040>.
- 591 [32] Richter T. O., van der Gaast S., Koster B., Vaars A., Gieles R., de Stigter H. C., de Haas H., van Weering
592 T. C. E. (2006) The Avaatech XRF Core Scanner: Technical description and applications to NE Atlantic
593 sediments, *New Techniques in Sediment Core Analysis*, **267**, 39–50.
594 <https://doi.org/10.1144/GSL.SP.2006.267.01.03>.
- 595 [33] Tjallingii R., Röhl U., Kölling M., Bickert T. (2007) Influence of the water content on X-ray fluorescence
596 core-scanning measurements in soft marine sediments, *Geochemistry, Geophysics, Geosystems*, **8**, 1–12.
597 <https://doi.org/10.1029/2006GC001393>.
- 598 [34] Moore D.M., Reynolds R.C. (1997) *X-Ray Diffraction and the Identification and Analysis of Clay
599 Minerals*, Oxford University Press, Oxford.
- 600 [35] Behar F., Beaumont V., De Penteadó B. (2001) Rock Eval 6 Technology: Performance and developments,
601 *Oil & Gas Sci. Technol.*, **56**, 111–134. <https://doi.org/10.2516/ogst.2001013>.
- 602 [36] Fayed L., Attewell P. B. (1965) A simplified, non-rigorous, tabular classification of clay minerals with
603 some explanatory notes, *Int. J. Rock Mech. Mining Sci.*, **2**, 271–276. [https://doi.org/10.1016/0148-
604 9062\(65\)90028-8](https://doi.org/10.1016/0148-9062(65)90028-8).

- 605 [37] Mac Kenzie R.C., Mitchell B.D. (1962) Differential Thermal Analysis, A review, *Analyst*, **87**, 420-434.
606 <https://doi.org/10.1039/AN9628700420>.
- 607 [38] Chantret F., Desprairies A., Douillet P., Jacob C., Steinberg M., Trauth N. (1971) Révision critique de
608 l'utilisation des méthodes thermiques en sédimentologie : cas des smectites (montmorillonites). *Bulletin du*
609 *Groupe français des Argiles*, **23**, 141-172. <https://doi.org/10.3406/argil.1971.1150>.
- 610 [39] Caillère S., Henin S., Rautureau M. (1982) *Minéralogie des argiles, 1. Structure et propriétés physico-*
611 *chimiques*, Masson, Paris, pp. 184.
- 612 [40] Smykatz-Kloss W. (1974). *Differential Thermal Analysis*, Springer Verlag, Heidelberg.
- 613 [41] Ptáček P., Kubátová D., Havlica J., Brandštetr J., Šoukal F., and Opravil T. (2010) The non-isothermal
614 kinetic analysis of the thermal decomposition of kaolinite by thermogravimetric analysis, *Powder Technology*,
615 **204**, 222-227. <https://doi.org/10.1016/j.powtec.2010.08.004>
- 616 [42] Sahnoune S., Saheb N., Khameh B., Takkouk Z. (2012) Thermal analysis of dehydroxylation of Algerian
617 kaolinite, *Journal of Thermal Analysis & Calorimetry*, **107**, 1067-1072. [https://doi.org/10.1007/s10973-011-](https://doi.org/10.1007/s10973-011-1622-6)
618 [1622-6](https://doi.org/10.1007/s10973-011-1622-6).
- 619 [43] Du L., Tian H., Wang W., Ding J., Wei X., Song M. (2017) Thermal stability of the eutectic composition
620 in NaCl-CaCl₂-MgCl₂ ternary system used for thermal energy storage applications, *Energy Procedia*, **105**,
621 4185-4191. <https://doi.org/10.1016/j.egypro.2017.03.892>.
- 622
623
624
625
626
627